Properties of Sediments from the New York/New Jersey Harbor

Keith W. Jones[1] and Huan Feng[2]

[1]Environmental Sciences Department, Brookhaven National Laboratory (kwj@bnl.gov)

[2]Department of Earth and Environmental Studies, Montclair State University

Sediments in the rivers, lakes and estuaries of the United States are widely contaminated by organic and inorganic compounds of anthropogenic origin. In many instances there is need for remedial action to ameliorate their environmental impact and potential risks to human health. In other cases, dredging is required to maintain and improve navigation channels used for commercial purposes. The New York/New Jersey Harbor is a specific example of a location where actions need to be taken to reduce the effects of contaminants for both environmental and practical reasons. For example, navigational dredging is required to maintain channel depths and for channel deepening to accommodate larger container ships. Approximately 1,500,000 m^3 of dredged material must be disposed of on upland locations each year. The Passaic River in New Jersey may require remediation for environmental reasons and indirectly, since it is a source of pollutants that can degrade sediment quality in other sections of the Harbor. Thus, there is a practical need to understand the properties of Harbor sediments and the behavior of associated contaminants in the environment in a way that integrates scientific investigations with the other features involved in creating a Harbor that meets environmental, recreational, and commercial needs.

We, and our collaborators, have carried out a number of investigations of the Harbor sediments using several different synchrotron-based analytical methods that are relevant to different aspects of the contaminated sediment problem. Our work has included use of four beam lines at the National Synchrotron Light Source and one beam line at the European Synchrotron Radiation Facility (ESRF). The experiments are discussed briefly below.

Knowledge of the microstructure of sediments can be useful in understanding sedimentation processes and the transport of contaminants by advection. Computed microtomography at NSLS beam line X27A was used to investigate the three-dimensional structure of a sandy sediment. The data are used to obtain values for the porosity as a function of depth through the sample and on the connectivity of the pore space. The results can be compared to theoretical models for the sedimentation process and used as the basis for modeling pore-scale contaminant advective-diffusive transport.

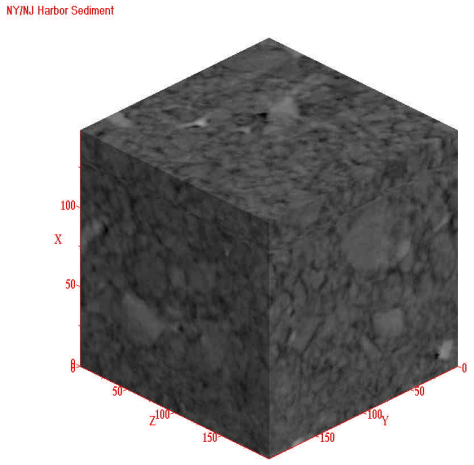

The distribution of metals on individual whole-sediment grains (diameters > 30 μm) was investigated with micro x-ray fluorescence at NSLS beam line X26A. The measurements showed that most of the grains

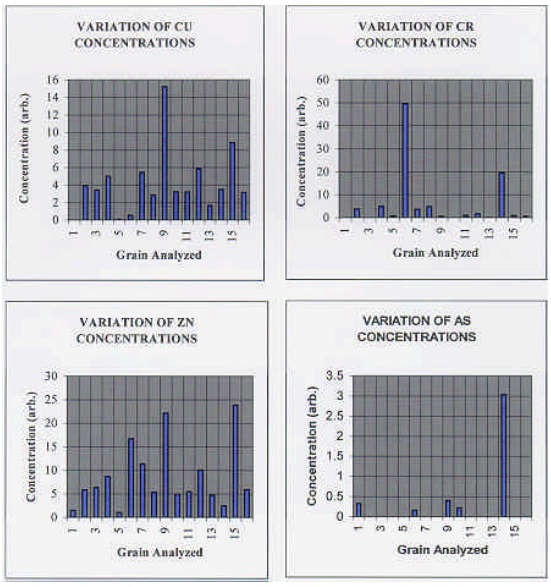

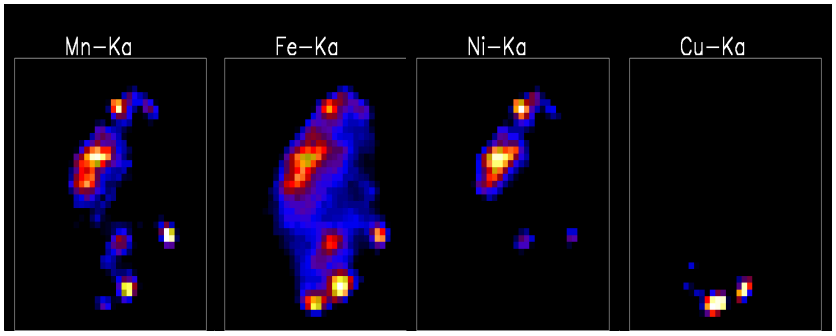

contained contaminants. Our results did not allow us to determine whether the contaminants were associated with the particle surface or with an organic film on the particle surface.

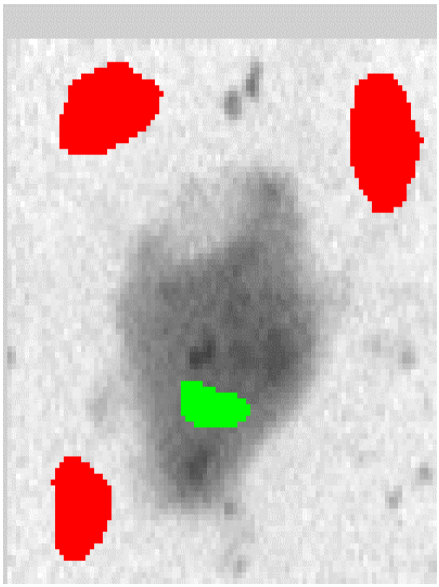

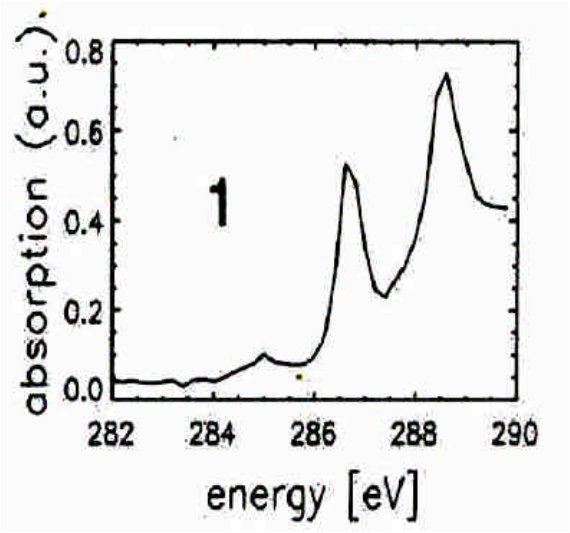

Further information on the metal distributions was obtained by study of single particle using fluorescent computed microtomography at the ID-13 beam line at the ESRF. Measurements were made on sediments from the Harbor and from the North Sea. Some elements were distributed through the particles while others were found on the surface and could be associated with smaller particles on the surface.

The relation of carbonaceous materials with respect to clay particles was investigated using scanning transmission x-ray microscopy at the NSLS X1A beam line. The measurements were made around the carbon K-x ray absorption edge. The results helped to give information on the morphology of the organic materials and sediments associated with them. The results may be useful in developing a better understanding of sediment-washing procedures designed to separate the organic materials from the sediment particles as part of a cleaning process. The functional groups of the organic compounds were investigated through x-ray near-edge spectroscopy measurements for carbon. Results indicate that Harbor organic materials give spectra substantially different from those obtained for humic substance standards.

We made further investigations of the functional groups occurring in the sediments using Fourier Transform Infrared Spectroscopy (FTIR) at the NSLS beam line U2B. Measurements were made on the raw sediments, on the liquids obtained from extraction with water, alcohol, and hexane, and on size fractions obtained after filtration to obtain size fractions <1.5 µm and <0.45 µm. The investigations demonstrated the heterogeneity of the sediments and for the materials extracted from them. Preliminary assignments of functional groups have been made to some spectral features. The results also show that application of FTIR could be useful for rapid assessment of the effectiveness of sediment washing decontamination technologies.

Finally, we used micro x-ray fluorescence at the NSLS beam line X26A to investigate mercury distribu-

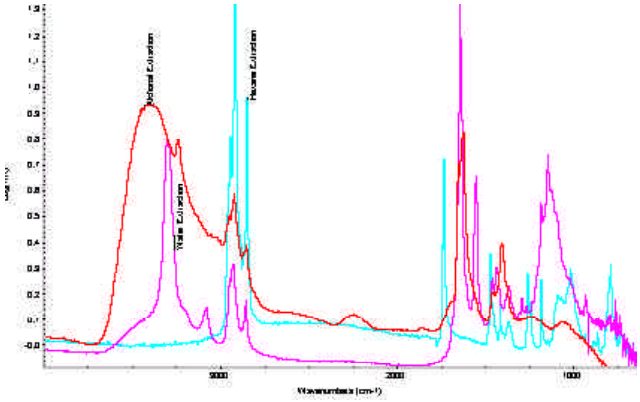

tions in the hair of subjects from two epidemiological studies. Mercury concentrations in the hair have been used to determine mercury intake from fish consumption in efforts to understand the magnitude of possible health effects on childhood development. The results will be useful in giving better spatial (time) resolution than possible with non-synchrotron x-ray sources and in understanding where the mercury resides in the hair structure. They will also help improve the data used in

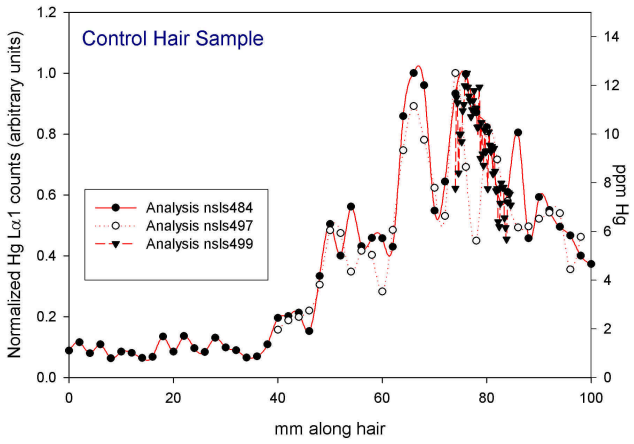

the epidemiological studies that are used to set limits on fish consumption. This is important for the Harbor since mercury levels there are affected by anthropogenic mercury sources.

We believe that the experiments discussed show that there are a number of synchrotron x-ray techniques that are useful for investigations of the complex sediment systems found in the New York/New Jersey Harbor. The experiments give information that is useful for understanding the characteristics of the sediments and associated organic and inorganic contaminants. The results have use in application of decontamination technologies, creation of beneficial use products, and setting of environmental regulations.

ACKNOWLEDGEMENTS

The experiments outlined here were carried out with a number of collaborators:

Brookhaven National Laboratory: E. Chouparova, Z. Song, S. Xu

Albert Einstein College of Medicine: N. S. Marinkovic

University of Chicago: A. Lanzirotti

European Synchrotron Radiation Facility: C. R. Riekel

University of Antwerp: L. Vincze, B. Vekemans, I. Szaloki, R. Van Grieken, F. Adams

State University of New York, Stony Brook: U. Neuhaeusler

University of Rochester: T. A. Clarkson

University of Southern Denmark: P. Grandjean

*Research supported in part by the US Department of Energy under Contract No. DE-AC02-98CH10886 and through Interagency Agreement DW89941761-01 between the US Environmental Protection Agency and the US Department of Energy.

Nature of Bone Mineral: Inception, Maturation, Aging

Lila Graham[1], Jonathan Hanson[2], Lisa Miller[3], Thomas Koetzle[2], Tatsuyuki Hori[1], Antonio Lanzirotti[4], Jenanan Vairavamurthy[3], and Melvin J. Glimcher[1]

[1]Dept. of Orthopedic Surgery, Laboratory for the Study of Skeletal Disorders and Rehabilitation, Harvard Medical School, Children's Hospital, Boston (lilagraham@cs.com)

[2]Chemistry Department, Brookhaven National Laboratory

[3]National Synchrotron Light Source, Brookhaven National Laboratory

[4]University of Chicago

The mechanical and physiological functions of bone as an ***organ***, a ***tissue*** and a ***substance*** are highly dependent on the chemistry, structure and spatial and chemical interactions of its major components: the inorganic crystals of Ca-P, the structural protein collagen, and non-collagenous proteins [1-12]. From the structural standpoint, the mechanical properties of ***bone substance*** result from the impregnation of the otherwise soft, pliable organic matrix of bone tissue by the rock-like but ***brittle*** Ca-P crystals of apatite which convert the soft matrix to a relatively rigid, two-phase or multiphase composite material whose combined properties are quite different from the simple algebraic sum of its components [5] [8-12].

Since "young" apatite crystals differ in their composition and structure from "old" apatite crystals, their capacity to function in biological processes and their contribution to the mechanical properties of bone substance and bone tissue will be a reflection of the age distribution of the crystals, which is a function of relative rates of bone formation and resorption (remodeling). An understanding of the changes in the mineral phase that occur after its initial deposition in the tissue (maturation of the crystals) is therefore essential for a correct interpretation of the overall changes in bone and mineral metabolism in metabolic disorders, genetic abnormalities and during repair and healing of bone. In the present work, special attention is focused on crystal maturation and the initial formation of the mineral phase, since the latter could provide important new information on the 3-D conformation and chemical footprint of the component(s) in the organic matrix that act as ***nucleation sites*** for the inorganic crystals.

There is increasing evidence that the apatite crystals of bone can interact with certain mesenchymal stem cells to induce proliferation and differentiation to osteoblasts and that their efficiency in this process is also dependent on the structure and organization of the crystals. Similarly, the efficacy of bone morphogenic proteins bound to apatite crystals is dependent on pore size, packing density, geometry, composition, and crystal structure of the apatitic preparation. Detailed structural data could eventually lead to the synthesis of materials that would either mimic the induction of proliferation and differentiation of osteoblasts by bone apatites, greatly assisting osteogenesis and mineralization, or inhibit ectopic calcification.

We are investigating the long- and short-range order of the initially deposited solid phase of Ca-P in fresh frozen bone by simultaneous wide-angle XRD, X-ray fluorescence (for Ca concentration) and simultaneous FTIR and X-ray fluorescence spectroscopy carried out *in situ* on intact bone. The samples are very small, whole intramuscular bones of freshly caught live herring and shad fish, immediately frozen in liquid N_2. A great advantage is that the fish bone can be scanned at very short intervals along the length of the bone starting from the wholly unmineralized portion to the initial site of calcification to maximum calcification. Also, previous EM studies had shown that collagen fibrils and crystals were both very highly oriented parallel to the long axis of the bone. Thus, the intensities of XRD reflections would be focused and low intensity peaks would be detected that might otherwise be missed in samples where the tissue is more randomly organized at the microscopic and ultrastructural levels. We have completed preliminary experiments to detect the initial mineral phase of fish bones by XRD with simultaneous Ca detection.

Despite suggestions that there are Ca-P solid phase precursors which are different from apatite and precede the formation of apatite, numerous studies by XRD, FTIR and ^{31}P NMR have not detected *a* ***solid crystalline phase*** other than apatite in bone. However, as we have pointed out [13], this does not preclude the initial formation of small amounts of transient solid phases that very rapidly dissolve and/or later undergo

solid-state transformation to apatites. There are biological and technical obstacles that have prevented a definitive solution of the structure of the initial Ca-P deposits [5, 14]. Firstly, even very mature bone crystals generate very poor XRD patterns as a result of both their nano-crystal size and poor crystal lattice perfection. This is even more evident as one examines progressively younger and younger bone crystals which generate only a few broad and poorly resolved XRD reflections from which a unique crystal structure cannot be deduced. Biologically, since in most bone tissue there is continuous turnover, a "gross" sample of bone is not homogeneous with respect to the age of the crystals in the usual bone specimen. Also, the Ca-P solid phase of the very earliest phases of mineralization constitutes only a very small proportion of the entire sample. As a result, spectral data generated by the mineral phase is overwhelmed and obscured or significantly distorted by spectra generated by the organic matrix components. We have overcome most of these problems in our initial studies carried out on the very thin (~0.3mm in diameter) intact intramuscular bones of herring and shad fish.

Initial studies were focused on methodology and specific adaptation of the synchrotron beam and other equipment, as well as the preparation and handling of the specimens, which permitted us to detect the earliest mineral phase deposited. We first identified the region were no mineral was detected, then proceeded along the length of the bone to where the mineral phase was clearly identified by XRD. We then translated back towards the unmineralized portion of the bone over very short distances to a region where the intensities of the XRD reflections were considerably reduced. This region was then bracketed until a region was pinpointed where XRD barely detected mineral phase and minimal further translation of the specimen and long exposure revealed no mineral phase (**Figure 1**). At this point the very youngest mineral phase of bone found to date was identified as a very poorly crystalline apatite. We were particularly interested in determining whether OCP (octacalcium phosphate) or other Ca-P mineral phases were present, since OCP has been postulated to be an early precursor phase of the mineral phase of bone. However, no OCP or other phase was detected despite the fact that the characteristic high intensity XRD reflection of standard OCP was easily observed.

A major goal is to be able to locate the following regions of bone: (i) totally unmineralized bone in which no Ca can be detected by X-ray generated fluorescence spectroscopy and no evidence of a mineral phase by FTIR and XRD; (ii) an immediately adjacent region where Ca is detected but there is no evidence of a mineral phase by FTIR and XRD; and (iii) an adjoining region where Ca and a mineral phase are both identified, the latter by FTIR and XRD or by FTIR alone, which is somewhat more sensitive than XRD. In any event, the adjacent region will almost certainly contain sufficient mineral phase to be detected by both FTIR and

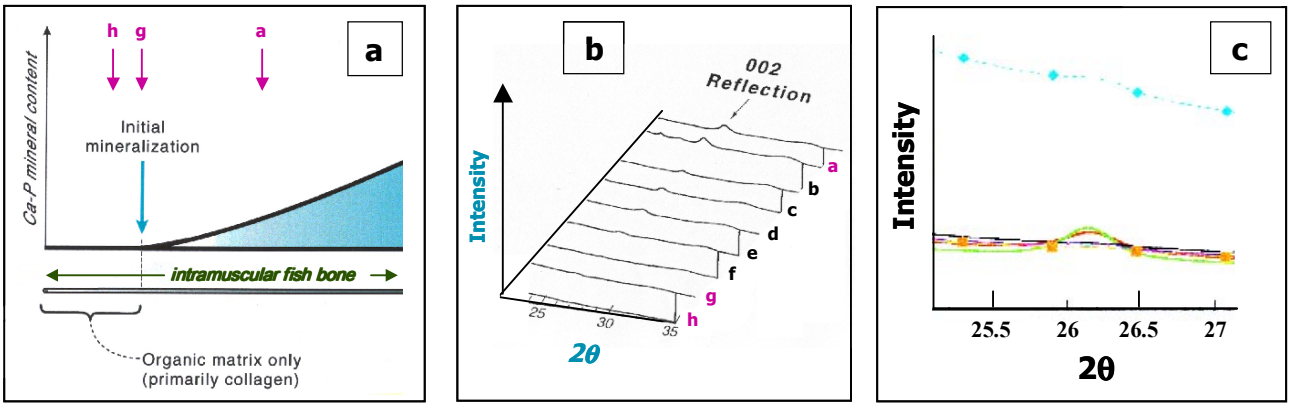

Figure 1: *(**a**) Diagrammatic sketch of intramuscular fish bone showing location of initial mineralization and progressive increase in mineral content along the length of the bone (**b**) X-ray diffractiometry of a specimen starting at a location with a very modest accumulation of mineral and proceeding towards the unmineralized portion (**c**) "Bracketing" in a similar sample at a location similar to (**h**) with much longer exposure times: blue curve is site of initial mineralization (displaced upward for clarity) – minimal further translation of the specimen towards the unmineralized region showed no mineral reflections (black line). Green and red line reflections are from regions of bone with slightly more mineral content than the initial site. Peaks shown are 002 reflections.*

XRD. The results of these experiments should not only allow us to characterize an even earlier stage of the bone mineral, but also to determine whether this younger mineral phase is an apatite or whether it is another mineral phase such as OCP. It will also allow us to chart the steps immediately preceding the formation of a solid mineral phase. In our first preliminary experiments we were successful in detecting all three stages using XRD and simultaneous X-ray generated fluorescence spectroscopy.

REFERENCES

1. Weiner, S. and Traub, W. (1992) *Bone structure: from angstroms to microns.* FASEB J **6**: 879-885.

2. Mann, S. and Weiner, S. (1999) *Biomineralization: structural questions at all length scales.* J Struct Biol **126**: 179-181.

3. Wagner, H. D. and Weiner, S. (1992) *On the relationship between the microstructure of bone and its mechanical stiffness.* J Biomech **25**((11)): 1311-1320.

4. Weiner, S. and Traub, W. (1989) *Crystal size and organization in bone.* Connect Tissue Res **21**: 259-265.

5. Glimcher, M. J. *The nature of the mineral phase in bone: Biological and clinical implications*. in *Metabolic bone disease and clinically related disorders, 3rd ed*. 1998. San Diego: Academic Press.

6. Glimcher, M. J. *Composition, structure and organization of bone and other mineralized tissues and the mechanism of calcification*. in *Handbook of Physiology 7: Endocrinology, vol VII*. 1976. Washington, D.C.: American Physiological Society.

7. Glimcher, M.J. (1984) *Recent studies of the mineral phase in bone and its possible linkage to the organic matrix by protein-bound phosphate bonds.* Philos Trans R Soc Lond B Biol Sci **304**(1121): 479-508.

8. Landis, W. J. (1999) *An overview of vertebrate mineralization with emphasis on collagen-mineral interaction.* Gravit Space Biol Bull **12**(2): 15-26.

9. Landis, W.J., Hodgens, K. J., and Arena, J. (1996) *Structural relations between collagen and mineral in bone as determined by high voltage electron microscopic tomography.* Microsc Res Tech **33**(2): 192-202.

10. Landis, W. J. (1996) *Mineral characterization in calcifying tissues: atomic, molecular and macromolecular perspectives.* Connect Tissue Res **34**(4): 239-246.

11. Landis, W.J. (1995) *The strength of calcified tissue depends in part on the molecular structure and organization of its constituent mineral crystals in their organic matrix.* Bone **16**(5): 533-544.

12. Christofferson, J. and Landis, W. J. (1991) *A contribution with review to the description of mineralization in bone and other calcified tissues in vivo.* Anat Rec **230**(4): 435-450.

13. Rey, C, Hina, A, and Glimcher, M J (1995) *Maturation of poorly crystalline apatites: Chemical and structural aspects in vivo and in vitro.* Cells and Materials **5**: 345-356.

14. Kim, H M, Rey, C, and Glimcher, M J (1995) *Isolation of calcium-phosphate crystals of bone by non-aqueous methods at low temperature.* J Bone Miner Res **10**(10): 1589-1601.

Element Mapping in 10 to 25 Micrometer Interplanetary Dust Particles

George J. Flynn

State University of New York at Plattsburgh (george.flynn@plattsburgh.edu)

Interplanetary dust particles (IDPs), like the one shown in **Figure 1**, range from 5 to 50 micrometers in size. The IDPs are dust from comets and asteroids collected from the Earth's stratosphere by high-altitude aircraft. Micrometeorites are larger dust particles, ranging from ~25 micrometers up to millimeters in size, collected at the Earth's surface — usually from polar ices or the seafloor.

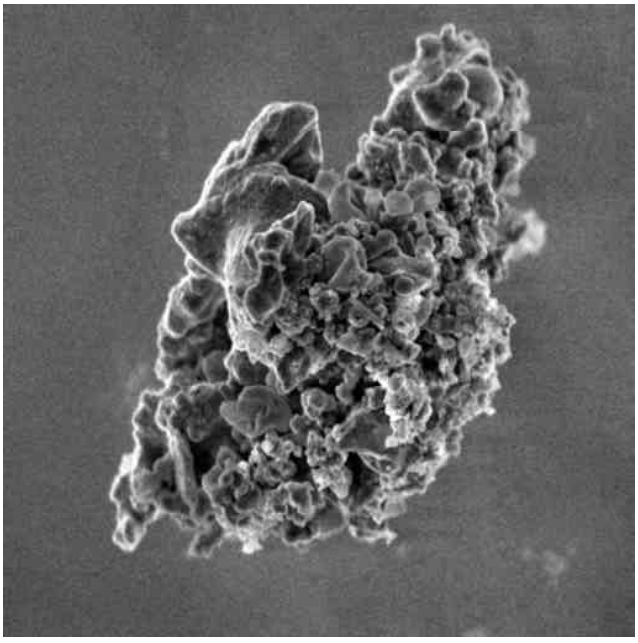

***Figure 1**: L2021C7, an ~10 micrometer IDP, recovered from the Earth's stratosphere.*

Using a synchrotron-based X-Ray microprobe we measured the chemical compositions of ~50 IDPs, and found enrichments in the moderately volatile elements relative to the most volatile-rich meteorites [1]. This result, coupled with the highly unequilibrated mineralogies and the excesses of D and ^{15}N reported by other investigators, indicates that anhydrous IDPs are the most primitive, i.e. least altered by thermal or aqueous processing, extraterrestrial materials currently available for laboratory analysis. Thus the composition, oxidization state and mineralogy of these primitive IDPs is likely to provide constraints on the conditions in the Solar Nebula at the time of dust formation. In addition, the carbonaceous matter in the IDPs is important because modeling by Anders [2] suggests that the IDPs may have carried a significant amount of pre-biotic organic matter, important for the origin of life, to the surface of the early Earth.

Using a Scanning Transmission X-ray Microscope (STXM) we mapped the spatial distributions of C, O, K, and Ca in IDPs, and C in micrometeorites with a spatial resolution of 50 to 100 nm. The C-mapping indicates that IDPs contain anywhere from a few wt-% up to 90 wt-% carbon, much more carbon than is found in the most carbon rich meteorites [3].

Once the carbon-rich spots were identified, we obtained X-ray Absorption Near Edge Structure (XANES) spectra of the carbon-rich spots to determine if the carbon in IDPs is dominantly organic or elemental. Almost all the carbon-rich regions of the IDPs exhibit two strong pre-edge absorption peaks (**Figure 2**): an absorption near 285 eV, characteristic of the C-ring structure, and an absorption near 288.5 eV, characteristic of the C=O functional group. While the C-ring occurs in both elemental carbon (graphite and amorphous carbon) as well as aromatic carbon, the detection of the carbonyl (C=O) in almost all the carbon-rich regions of IDPs demonstrates that much of the carbon in these particles is organic [3]. This suggests that the amount of organic matter contributed to the early Earth

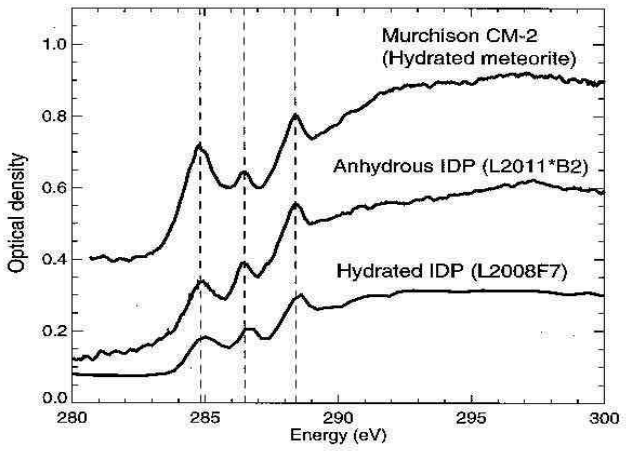

***Figure 2**: C-XANES spectra of two IDPs, L2011*B2 and L2008F7, and the Murchison carbonaceous meteorite.*

by extraterrestrial dust was substantial.

Oxygen mapping simply showed that O is contained in both the organic matter and the silicates. However, O-XANES on the C-rich regions confirmed the presence of carbonyl in IDP organic matter.

In most IDPs all the carbon-rich regions detected in the untramicrotome sections had the same C-XANES spectrum, indicating that only one type of carbon was present. This observation allowed us to perform FTIR spectroscopy on the larger mass of material remaining after a few slices were prepared by ultramicrotomy to further characterize the organic carbon in IDPs. By FTIR we were able to identify C-H stretching absorption (**Figure 3**), demonstrating the presence of aliphatic hydrocarbons in the IDPs [3]. The major minerals, anhydrous silicates, clays, oxides, carbonates, etc., in the IDPs interfere with the detection of other organic functional groups by FTIR. However, we have recently performed FTIR spectroscopy on IDPs that were etched using hydrofluoric acid to remove the major minerals, and we observed the carbonyl functional group by FTIR [4].

We found carbon with very similar C-XANES and FTIR spectra, but at lower concentrations, in micrometeorites recovered from Antarctic ice. These micrometeorites, which are larger than the IDPs, were expected to carry little or no organic matter to the Earth's surface because they are heated more severely during atmospheric deceleration.

K and Ca were mapped in anhydrous IDPs, to avoid the effect of element mobilization during the aqueous alteration experienced by hydrated IDPs. The K-mapping indicated that in one K-rich IDP the K was concentrated in the silicates, which dominate the IDP, while the Ca-mapping showed only a few submicron-sized Ca hot-spots, indicating that Ca is in a minor phase in the IDP.

Determining the host phase(s) of the minor elements is important to the understanding of the conditions under with the minerals in the IDPs formed and the alteration IDPs experience from heating during atmospheric deceleration. To understand the element distribution, we performed x-ray fluorescence microtomography, producing 3-dimensional maps of the distributions of Fe, Ni, Zn, Sr, and Br in individual, intact IDPs [5]. In one IDP, we found two regions of high Zn and only one small Sr-rich spot, demonstrating that both elements are concentrated in minor phases in these IDPs.

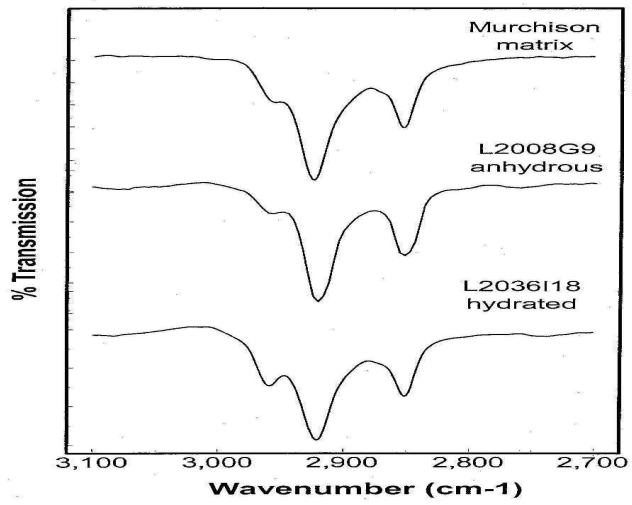

***Figure 3**: FTIR spectra of two IDPs, L2008G9 and L2036I18, and the Murchison carbonaceous meteorite. The absorptions are CH_2 and CH_3 and stretching features.*

REFERENCES

[1] G. J. Flynn et al., in Analysis of Interplanetary Dust, AIP Press, New York, 291 (1996).

[2] E. Anders, Nature, 1989.

[3] G. J. Flynn et al., in A New Era in Bioastronomy, ASP Conf. Proc., Vol 213, 191 (2000).

[4] G. J. Flynn et al., *Lunar and Planetary Science XXXIII*, LPI, Houston, CD-ROM, Abstract #1320 (2002).

[5] S. R. Sutton et al., Lunar & Planet.Sci.XXXI, Lunar & Planet. Inst., CD-ROM, Abs #1857. (2000).

Infrared and X-ray Probes of Materials Under Pressure: Spectroscopy, Diffraction, and Imaging

Russell J. Hemley, Zhenxian Liu, Jingzhu Hu, Quanzhong Guo, and Ho-kwang Mao

Geophysical Laboratory, Carnegie Institution of Washington (hemley@gl.ciw.edu)

Understanding the effects of pressure on materials is fundamental to an expanding range of problems in the physical and even biological sciences [1, 2]. Arguably, synchrotron radiation techniques have become the most important category of methods for characterizing materials at very high pressures, including megabar pressures (>100 GPa) and at variable temperatures from cryogenic conditions to >5000 K using a variety of devices based on the diamond-anvil cell. Because of the significant enhancement in our ability to probe microscopic samples provided by this source, the high brightness of IR radiation from the VUV ring of the NSLS is ideally suited to studies of materials under extreme pressures [3]. This facility is complemented by the high-pressure/microdiffraction x-ray beamlines X17C (the first synchrotron facility dedicated to high-pressure materials studies) and X17B [4]. All three beamlines, which are supported by a sample preparation and off-line characterization lab, have led to numerous discoveries about the evolution of materials under pressure. Together the beamlines provide a unique environment for performing multiple and complementary measurements required for full characterization of phenomena as a function of pressure and temperature.

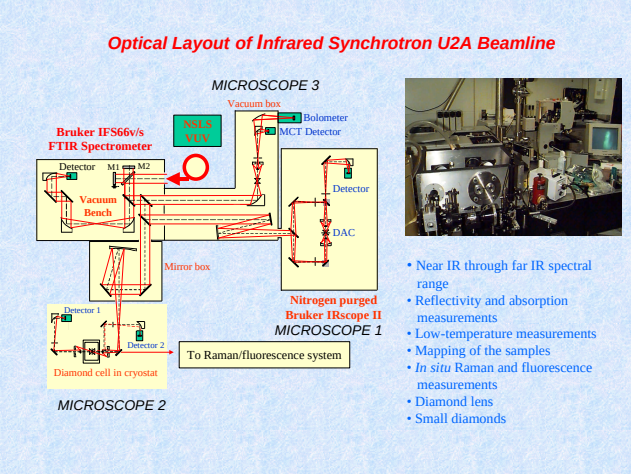

Figure 1. *U2A beamline layout.*

The dedicated high-pressure IR beamline U2A is an integrated facility for a wide range of microspectroscopic studies from ambient to ultrahigh pressures (1 bar to >300 GPa) and at variable temperature (2 to 1200 K in a diamond cell; to 1800 K at 1 bar) [3]. It includes a Bruker IFS-66v FT-IR spectrometer capable of operating at 10 to 25,000 cm^{-1} coupled to the synchrotron source with 40 x 40 mrad aperture. The optics includes a commercial Bruker IRscope II infrared microscope operating in the near- and mid-IR range and two custom long-working distance microscopes. At the beamline, one can perform:

- Diffraction-limited micro far-IR absorption measurements.
- IR absorption/reflectivity measurements over a broad range of pressures (e.g., to >200 GPa), including both polycrystalline and single-crystal studies.
- Companion micro-Raman, visible absorption/emission/reflectivity, and ruby fluorescence spectra. Using kinematic mounts, the system can be easily switched for measurements with visible lasers (argon-ion 457-514.5 or 700-950 nm Ti:sapphire) and single stage spectrographs equipped with interchangeable gratings and CCD array detectors.
- Low-temperature (*l*-He) studies at ultrahigh pressures. A specially designed long piston cylinder diamond cell is placed inside a continuous flow cryostat with the cell in an atmosphere of exchange gas for efficient temperature operation.
- IR/visible imaging studies of ambient- and high-pressure samples (e.g., mineral petrography).

The facility at X17 is built around an x-ray microprobe used extensively for high-pressure experiments, primarily x-ray diffraction [4]. Beams are either collimated with multiple slit systems or focused with Kirkpatrick-Baez mirrors down to <10 μm. This is crucial for both mapping distributions of pressure, stress, phases, sample heterogeneity over a broad range of pressures, probing multiple phases for cross-calibration studies, and measurements of <10 μm samples at ultrahigh pressures (>300 GPa). With x-ray transparent gaskets (and diamond-cell assemblies) made of

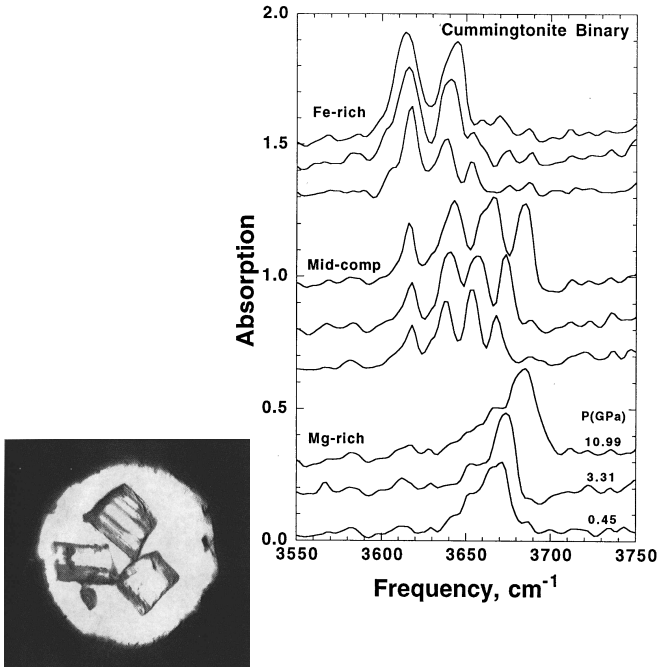

***Figure 2**. Spatially resolved single-crystal high-pressure IR measurements of the mineral cummingtonite of different compositions (a) shown in a diamond cell as a function of pressure (view ~300 mm), (b) together with spectra of the individual crystals indicating the existence of a pressure-induced phase transition [5].*

materials such as Be, one can probe samples over a wide range of solid angles with respect to the loading axis; diffraction measurements under these conditions can allow imaging of the strain, stress, strength, and texture development in the sample as a function of applied pressure. With wide-access diamond-cells, single-crystal x-ray diffraction experiments can be performed even on multiple crystals within the cell. For these experiments, energy dispersive x-ray diffraction probes excellent spatial resolution, because of the ability to collimate signal on the diffracted as well as the incoming beam. X-ray radiographic measurements can also be performed with these small beams to provide measurements of macroscopic deformation and equations of state (e.g., for liquids and amorphous materials). Finally, ambient-temperature studies are complemented by both cryogenic studies (<10 K) as well as in situ double-sided laser heating/x-ray diffraction measurements. These experiments have been developed over the past ten years at the dedicated X17C beam line. The variable-temperature experiments have been performed part-time at X17B; during the coming year, the equipment will be set up permanently at the new dedicated X17B3 facility.

REFERENCES

[1] R.J. Hemley and N.W. Ashcroft, Physics Today, 51, 26-32 (1998).

[2] R.J. Hemley, G. Chiarotti, M. Bernasconi, and L. Ulivi (eds). *High-Pressure Phenomena, Proceedings of the International School of Physics "Enrico Fermi"* (North Holland, New York, 2002) in press.

[3] R.J. Hemley, A.F. Goncharov, R. Lu, M. Li, V.V. Struzhkin and H.K. Mao, II Nuovo Cimento D 20, 539-551 (1998); Z. Liu et al., to be published.

[4] Hu, J, H.K. Mao, Q. Guo, and R.J. Hemley, X-ray diffraction studies at X17C of the NSLS. In *Science and Technology of High Pressure*, edited by M.H. Manghnani, W.J. Nellis, and M. Nicol (Universities Press, Hyderabad, India, 2000) pp. 1039-1042.

[5] H. Yang, R.M. Hazen, C.T. Prewitt, L.W. Finger, R. Lu and R.J. Hemley, Am. Mineral. 83, 288-299 (1998).

[6] R.J. Hemley and H.K. Mao, Internat. Geol. Rev. 43, 1-30 (2001).

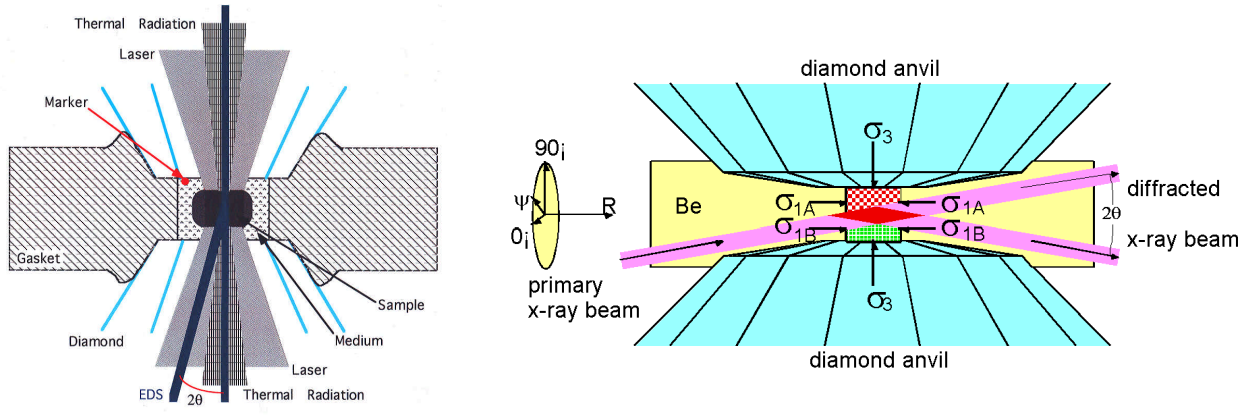

***Figure 3**. Schematic of (left) the double-sided laser heating/x-ray diffraction technique in the diamond-anvil cell, and (right) the radial x-ray diffraction method [6]*

Determining Surface Site Preferences for Metal Uptake by Micro-XRF

Richard J. Reeder

Department of Geosciences, State University of New York at Stony Brook (rjreeder@sunysb.edu)

One of the important controls on the mobility and fate of metal species dissolved in natural waters is interaction with surfaces of mineral grains that compose soils, sediments, and aquifer materials. Uptake via adsorption or coprecipitation removes metals from aqueous solutions, thereby restricting their transport and, in some cases, their bioavailability. This effect may be desirable in the case of toxic metal species, but it may alter biogeochemical cycles of nutrients and other metals. The mechanism and effectiveness of uptake depend on the particular metal as well as a number of other factors, including the aqueous metal speciation, the solution chemistry, and surface properties of the solids present. Among the more difficult aspects to characterize are the distribution and availability of reactive surface sites on minerals and their influence on adsorption and coprecipitation. Low symmetries of many common minerals and the tendency of some minerals to exhibit multiple forms (i.e., faces) allow for the existence of multiple sites for attachment at their surfaces. The occurrence of sites of preferential attachment on specific faces or in surface features such as growth steps may result in a spatial segregation of distinct sites into separate regions of the mineral surface. The significance of this heterogeneous distribution of different sites is illustrated by the tendency of metals to interact differentially between nonequivalent sites. Important examples include the preferential sorption of some metals on edge sites relative to basal plane sites of clays and the differential incorporation of metals between nonequivalent growth steps on common minerals such as calcite and apatite (Reeder and Rakovan, 1999).

Characterization of site preferences for various metals interacting with mineral surfaces is possible when (1) regions of the mineral surface onto which the distinct site have been spatially segregated are large relative to the beam size of the analytical probe and (2) the difference in elemental concentration is large relative to the precision of the method. In this chapter, I provide an example of how surface site preferences of three metals (Co^{2+}, Zn^{2+}, and Cu^{2+}) interacting with the common $(10\bar{1}4)$ growth surface of calcite ($CaCO_3$) can been characterized using synchrotron micro-X-ray fluorescence techniques. Details of this method, including the relevant considerations of beam size and analytical precision, have been described by Lanzirotti in "Hard X-Ray Microprobe."

The $(10\bar{1}4)$ surface of calcite commonly grows by the spiral mechanism (Paquette and Reeder, 1995) in which monolayer steps advance around the site of emergence of a dislocation (Burton et al., 1951). The anisotropy of the calcite structure along the $(10\bar{1}4)$ plane causes steps to form preferentially parallel to the equivalent directions $[\bar{4}41]$ and $[48\bar{1}]$, resulting in a growth spiral composed of polygonized regions (i.e., vicinal faces) having growth steps moving along the surface in distinct directions. Surface symmetry requires that steps parallel to the same direction but moving in opposite directions are nonequivalent. This nonequivalence results from the difference in coordination geometry of the calcium sites exposed in the different steps. As a result, spiral growth on this surface of calcite produces two pairs of vicinal faces, which contain steps and incorporation sites that are structurally different. **Figure 1** illustrates the difference between nonequivalent steps on the calcite $(10\bar{1}4)$ face; the detailed structural differences between the sites in these nonequivalent steps have been described elsewhere (Staudt et al., 1994; Paquette and Reeder, 1995; Reeder and Rakovan, 1999).

To assess the preferences for incorporation of metals among these distinct surface steps, calcite single crystals were grown under controlled conditions; a metal dopant (Co^{2+}, Zn^{2+}, or Cu^{2+}) was introduced allowing uptake preferences to be recorded as the dopant is incorporated into surface layers produced during spiral growth. Recovered calcite crystals may be as large at 800 μm across and were sectioned parallel to a $(10\bar{1}4)$ face exhibiting a single growth spiral, retaining the as-grown surface. Sections were typically 20-30 μm in thickness, and roughly correspond to the final layers added to a single $(10\bar{1}4)$ face. The regions corresponding to the nonequivalent vicinal faces may be as large as 200 x 200 μm. An incident beam size ranging from 5 x 5 μm to 10 x 15 μm easily allows "mapping" the elemental distribution within and between the adjacent vicinal faces on the same crystal face. Given the

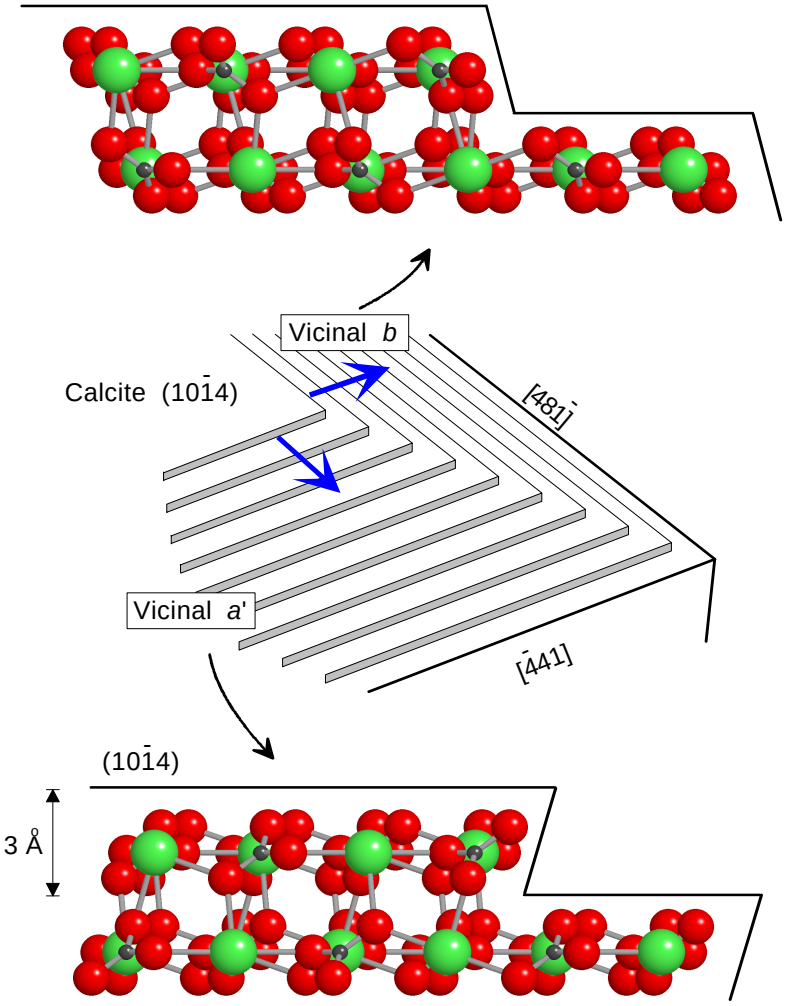

Figure 1. *Models showing structures of nonequivalent growth steps occurring on adjacent vicinal faces on the calcite (1014) surface.*

low X-ray absorption coefficient of $CaCO_3$ for energies spanning the *K*-edges of Co^{2+}, Zn^{2+}, and Cu^{2+}, the incident beam penetrates the entire section of the single crystal. Consequently, the actual spatial resolution is determined in part by the sample thickness and the angle of the incident beam relative to the crystal section (typically 45°).

Figure 2 shows maps of the distribution of Co^{2+}, Zn^{2+}, and Cu^{2+} among the vicinal faces of $(10\bar{1}4)$ surfaces of different calcite single crystals (Elzinga and Reeder, 2002). Orientations of the single crystals are the same in each image. The hot colors (e.g. red) correspond to highest metal concentrations and the cold colors (blue, black) correspond to lowest metal concentrations. For all images, the metal concentration is roughly uniform within a given vicinal face and between equivalent vicinal faces, showing only minor gradients, sometimes associated with sample thickness. However, significant and sharply defined differences in concentration occur between nonequivalent vicinal faces, which document the preferential uptake of the metal between sites occurring in the nonequivalent steps composing the different vicinal faces.

A notable observation among these images (**Figure 2**) is that the preference for vicinal faces shown by Co^{2+} is opposite the preferences shown by Zn^{2+} and Cu^{2+}. This indicates that these metals show different preferences among the nonequivalent surface steps and sites, despite having similar formal charges and ionic radii. Related studies involving EXAFS spectroscopy confirm that the structures of the surface complexes differ for these metals sorbed at calcite surfaces.

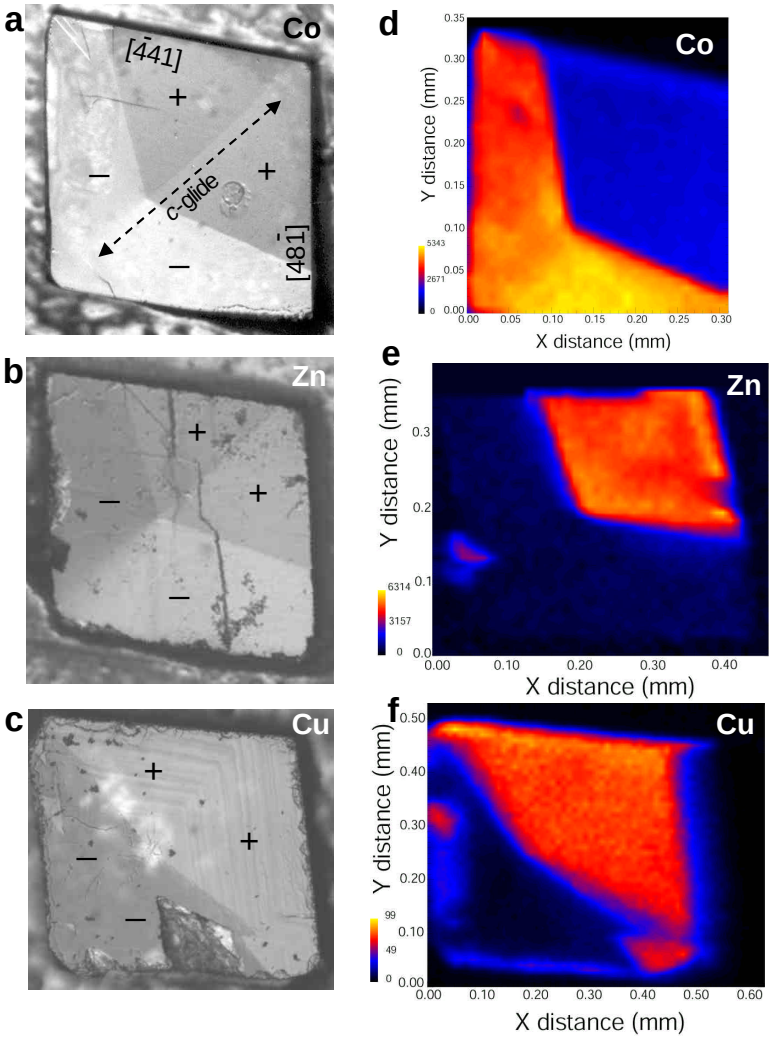

Figure 2. *Images of as-grown surfaces of calcite single crystals doped with (a) Co^{2+}, (b) Zn^{2+}, and (c) Cu^{2+}. The labels + and - indicate equivalent vicinal faces. Corresponding micro-XRF elemental maps (d-f); colors show relative differences in metal concentration between vicinal faces. (From Elzinga and Reeder, 2002)*

Studies that allow determination of surface site preferences provide direct insight to reaction mechanisms that control the behavior of many dissolved metals in natural systems. Synchrotron-based micro-XRF techniques offer one of the best methods for spatially resolved elemental mapping. Combined X-ray absorption spectroscopy also permits information to be obtained about coordination and oxidation state.

REFERENCES

Burton W.K., Cabrera N. and Frank F.C. (1951) The growth of crystals and the equilibrium structure of their surfaces. Roy. Soc. London Phil. Trans. A243, 299-358.

Elzinga, E.J. and Reeder, R.J. (2002) EXAFS study of Cu2+ and Zn2+ adsorption complexes at the calcite surface – Implications for site-specific metal incorporation preferences during calcite crystal growth. Geochim. Cosmochim. Acta (in press)

Paquette, J. and Reeder, R.J. (1995) Relationship between surface structure, growth mechanism, and trace element incorporation in calcite. Geochim. Cosmochim. Acta, 59, 735-749.

Reeder, R.J. and Rakovan, J. (1999) Surface structural controls on trace element incorporation during crystal growth. *In* Growth, Dissolution and Pattern Formation in Geosystems, B. Jamtveit and P. Meakin (eds.) Kluwer Academic, p. 143-162.

Staudt, W.J., Reeder, R.J., and Schoonen, M.A.A. (1994) Surface structural controls on compositional zoning of SO42- and SeO42- in synthetic calcite single crystals. Geochim. Cosmochim. Acta, 58, 2087-2098.